Non-contact damage monitoring technique for FRP laminates using guided waves

Mohit Garg[*1], Shruti Sharma[2], Sandeep Sharma[1] and Rajeev Mehta[3]

[1]*Department of Mechanical Engineering, Thapar University, Patiala, Punjab, India*
[2]*Department of Civil Engineering, Thapar University, Patiala, Punjab, India*
[3]*Department of Chemical Engineering, Thapar University, Patiala, Punjab, India*

Abstract. A non-contact, in-situ and non-invasive technique for health monitoring of submerged fiber reinforced polymers (FRP) laminates has been developed using ultrasonic guided waves. A pair of mobile transducers at specific angles of incidence to the submerged FRP specimen was used to excite Lamb wave modes. Lamb wave modes were used for comprehensive inspection of various types of manufacturing defects like air gaps and missing epoxy, introduced during manufacturing of FRP using Vacuum Assisted Resin Infusion Molding (VARIM). Further service induced damages like notches and surface defects were also studied and evaluated using guided waves. Quantitative evaluation of transmitted ultrasonic signal in defect ridden FRPs vis-à-vis healthy signal has been used to relate the extent of damage in FRPs. The developed technique has the potential to develop into a quick, real time health monitoring tool for judging the service worthiness of FRPs.

Keywords: fiber reinforced polymer composites; guided waves; damage localizations; structural health monitoring; lamb waves; VARIM; defects

1. Introduction

Fiber reinforced polymer (FRP) composites have been extensively used in the modern world due to their unique properties such as high strength-to-weight ratio, corrosion and thermal resistance. These properties are desirable for various applications like airplane and marine structures, automobile chassis and sporting goods. The use of FRP for naval application was initially driven by the need of easily fabricated composites having lightweight, strong, corrosion resistant, high durability, low thermal conductivity and lesser maintenance costs as compared to conventional materials like aluminum alloys and various types of steel etc. These composites are used to make various structural parts (like hull, decks etc.) in both commercial and military naval vehicles. Under such applications, the composites are exposed to extreme service conditions leading to high risk of deterioration. The environmental degradation and service related factors affect the fiber-matrix interfacial bonding which results in deteriorating its structural performance. The common damage behavior exhibited by FRP components under harsh service conditions

---

∗Corresponding author, Lecturer, E-mail: mohitgarg@thapar.edu

includes transverse micro-cracking, fiber-breakage and delamination. Initially, the ply failure begins with transverse micro-cracking through its thickness followed by delamination and lastly by fiber breakage. Growth and propagation of such damages in composites is very complex and depends on various factors such as constituent materials, fiber orientation, stacking sequence, exposure conditions etc. (Sihn *et al.* 2007). In addition to service induced damages some defects may be inherently present in FRP composites during manufacturing phase. Commonly observed manufacturing defects include air gaps, debonding, and non-uniformity of matrix. Presence of such defects in FRPs reduces their performance and durability.

Several techniques such as lock-in and transient thermography (Chaki *et al.* 2015, Palumbo *et al.* 2016), acoustography (Chaki *et al.* 2015), laser ultrasonics (Pistone *et al.* 2013, Hong *et al.* 2015), and shearography (Hung *et al.* 2000, De Angelis *et al.* 2012, 2015) have been proposed by various researchers for damage detection in composites. However, for naval applications, the regular assessment of composites in submerged condition is inhibited by the conventional damage inspection tools due to economic constraints such as high out-of-service costs linked with frequent monitoring schedules and also time consuming process associated with the removal of structures prior to their inspection. As a result, it exposes such structures to the risk of unnoticed fatal damages with huge loss of human life and property. Ultrasonic guided waves have been suggested as an effective structural health monitoring tool by various researchers to detect damages such as delamination, cracks etc. in FRPs (Benammar *et al.* 2008, Miao *et al.* 2012, Putkis *et al.* 2016).

Guided waves exploit the geometrical boundary (e.g., tube, cylinder or plates etc.) of the structure as a guiding surface for wave propagation. In the structures with a plate or sheet geometry, guided waves are called Lamb waves. These are complex vibrational waves that propagate parallel to the surface throughout the thickness thus scanning the entire thickness of the plate. Propagation characteristics are dependent upon the density, elastic properties, geometry of the structure and frequency of excitation. Lamb waves are characterized by longer propagation, lower attenuation, economical implementation, high sensitivity to structural damages and to the material in-homogeneities, ease of generation and acquisition of signals (Wilcox *et al.* 1999, Na and Kundu 2002) as compared to ultrasonic bulk waves. Owing to these characteristics, Lamb waves have been widely used by various researchers for damage detection in FRPs (Ramadas *et al.* 2011a, Liu *et al.* 2012, Moll *et al.* 2012, Providakis *et al.* 2014, Harb and Yuan 2016).

In most of the reported works, contact probes have been used to generate guided waves. The key obstacles in implementing contact transducers are: inadvertent variations in contact pressure affecting the repeatability of results, difficulty in generating specific Lamb wave mode and finally, the possibility of local damage due to use of contact probes. Few studies have attempted to generate Lamb waves in FRP composites by using either air-coupled (Castaings and Hosten 2001, Ramadas *et al.* 2011b, Liu *et al.* 2013, Chakrapani and Dayal 2014, Harb and Yuan 2016) or fluid coupled (Ben *et al.* 2013) non-contact ultrasonic transducers. The use of air/fluid coupling ultrasonic transducers also has several limitations such as: difference in mechanical impedance between air/fluid and the sample under investigation resulting in low precision, removal of the structure from its service conditions in-order to access the structure from both the sides and relatively less-effective technique for detecting near-surface damages. Another group of researchers (Rizzo *et al.* 2010, Pistone *et al.* 2013, Rizzo *et al.* 2015, Pistone and Rizzo 2015, Bagheri and Rizzo 2016) developed an ultrasonic guided wave set-up that could fine tune the incident angle and exploit specific Lamb wave mode to detect damages in submerged steel plates and underwater pipes. Recently, Sharma and Mukherjee (2014, 2015a,b) provided a real-time health monitoring methodology for monitoring corrosion in submerged steel plates using specific

leaky Lamb waves. Although considerable progress has been made in using Lamb waves for damage detection in various structural applications but research on their use for health monitoring of FRPs laminates is limited.

Nowadays, since the FRP composites are replacing conventional steel/aluminum (or their alloys) for naval structures, it is imperative to develop their real-time health monitoring methodology in a submerged state using an advanced technique which can replace the conventional methods of testing. The present study is an attempt to ultrasonically monitor defects encountered in FRP laminates using a non-contact, mobile and real-time guided wave technique. The main objective of this research is to develop a novel, non-destructive, in-situ and real-time experimental method for quick detection of manufacturing and in-service defects in FRP laminates by using a pair of transducers in pitch-catch orientation, specifically used for underwater applications. Specific Lamb wave modes are generated by exploiting the submerged state of FRPs, wherein water is used as a natural couplant.

Lamb waves are usually excited by impinging the plate obliquely with an ultrasonic signal emitted by a high frequency transducer. As a result, variety of different waves are produced on excitation inside the material, which is followed by the superposition of longitudinal and shear waves in a thin plate with an infinite number of modes for both symmetric and anti-symmetric displacements within the layer. The wave propagation characteristics vary with the incident angle, excitation and structural geometry. For the damage detection in FRPs such as cracks, delamination, missing fiber etc., a mode specific to the aforementioned defects needs to be excited. Desired Lamb wave mode in pitch-catch orientation can be selectively excited by arranging the transducers at a specific angle with respect to the specimen plate geometry. The incident angle, 'θ', necessary to produce a desired Lamb wave can be calculated from Snell's law as given below

$$\theta = \sin^{-1}\left(\frac{V_L}{V_{Ph}}\right) \tag{1}$$

where, V_L = longitudinal velocity of the incident wave in coupling media

V_{Ph} = phase velocity of desired Lamb wave mode

In the present study, for monitoring of submerged FRP specimens, water acts as a natural coupling medium. The preferred Lamb waves (other modes being suppressed) have been experimentally determined by using normal beam transducers in a pitch-catch orientation.

2. Experimental

2.1 Set-up and specimen details

Experimental set-up comprised of an acrylic tank of dimensions (1500 mm x 1000 mm x 900 mm) filled with water to a depth of 700 mm. FRP specimen fabricated by Vacuum Assisted Resin Infusion Molding (VARIM) technique was fully immersed in water and placed in duly supported position. Figs. 1(a) and 1(b) show the actual and schematic arrangement of the experimental set-up. Two holders designed to hold normal beam transducers, were assembled on top of the tank. Pair of transducers were placed in a pitch-catch orientation. This set-up exhibited four degrees of freedom (X,Y, Z, θ) over the submerged specimen as shown in Fig. 1(a).
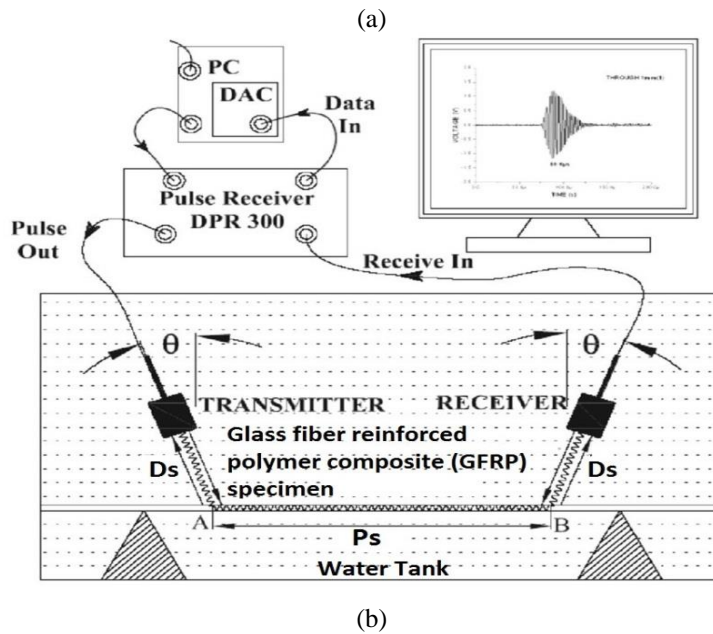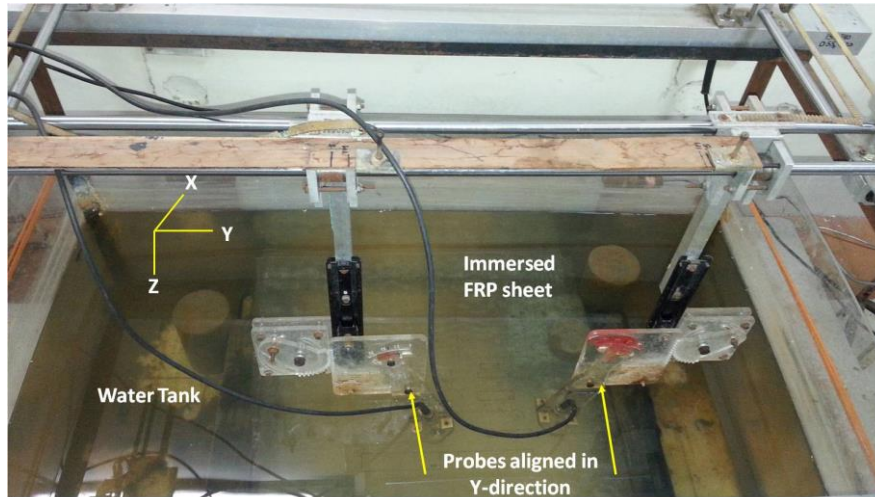
(a)

(b)

Fig. 1 Experimental set-up (a) Actual and (b) Schematic arrangement

For ultrasonic investigations, an ultrasonic transmission (UT) system consisting of a Pulser-Receiver (PR) device (JSR make, Model DPR 300), ultrasonic transducers (Panametrics[TM] Immersion Probes) (as shown in Fig. 2), data acquisition system (Agilent make) and display devices were used. Pair of immersion probes (Model No. A301S, Olympus Panametrics NDT) with a central frequency of 0.5 MHz were used in the present study. A lower frequency ultrasonic transducer is preferred for damage evaluation in thin FRP plates due to lesser material attenuation, scattering and mode conversions at lower frequencies as compared to higher frequencies.

Fig. 2 Ultrasonic set-up

Probes were arranged at the same angle with vertical (θ) in order to make the receiver transducer more sensitive to the wavelength of input frequency while subduing noises (Fig. 1(b)). The longitudinal waves generated by the transmitter probe travel through the surrounding water and impinge obliquely the surface of the laminate sheet. Desired Lamb wave mode can be generated by varying the angle of incidence (θ).

Another experimental parameter is the distance of separation (D_s) of probe and submerged sheet as shown in Fig. 1(b). It is the distance travelled by the guided wave prior to its interaction with the submerged specimen. In this study, distance of separation was adjusted in terms of time of flight of longitudinal waves in water (t_s) in Pulse Echo (PE) mode. Both the transducers were placed with same D_s using PE signatures. This set-up was used for generating Lamb waves in Pulse Transmission (PT) configuration wherein longitudinal wave front generated by transmitter interacts obliquely with the specimen and receiver probe detects the propagating leaky Lamb waves through fluid coupling on the other end. The distance of Lamb wave propagation through the specimen is termed as propagation span (P_s) as shown in Fig. 1(b).

To develop an effective monitoring strategy for FRP sheets, good signal fidelity is a must. It was observed experimentally that large D_s resulted in excess loss of incident energy to the surrounding water and yielded a weak UT signal in PT mode. Also, too small a value of D_s resulted in field reflections that tend to superimpose over the initial ultrasonic signal. Thus, a suitable D_s and corresponding t_s for use in subsequent experiment had to be chosen.

Fig. 3(a) shows the received signal amplitudes (V_p) obtained by using t_s of 30 μs and 40 μs while keeping other experimental parameters like P_s, θ and PR settings same. The trend of V_p with varying t_s (Fig. 3(b)) clearly shows that V_p is approximately 20% greater when t_s is set at 30 μs as compared to 40 μs. Hence, for the subsequent experimental investigations both the probes were set at a t_s of 30 μs.
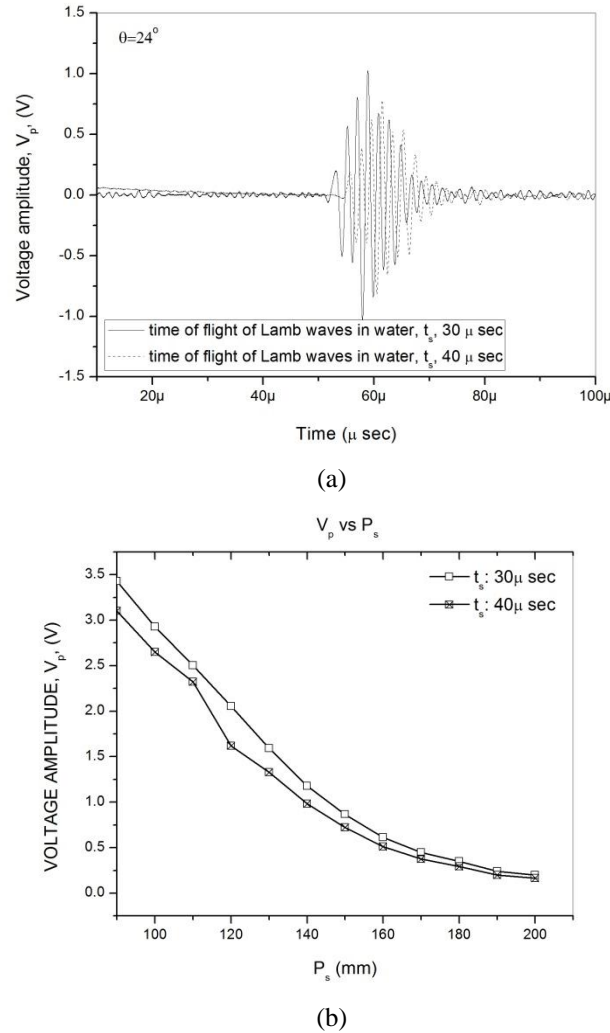
(a)

(b)

Fig. 3 Effect of time of flight of guided wave in water medium (a) Specimen PT signature and (b) Trends of transmitted voltage amplitudes with varying propagation span for $\theta = 24^{o}$

2.2 Selection of optimum angle (θ)

Lamb waves exhibit multi-mode behavior wherein each mode has a unique way of interaction with the defects in the specimen. Various researchers (Liu *et al.* 2001, Hay and Rose 2002, Sharma and Mukherjee 2014, 2015a,b) have experimentally determined specific guided wave modes for effective health monitoring in pipes, rods, plates etc. Desired Lamb wave mode must exhibit distinct and sharp waveform with good signal fidelity and repeatability, so that interaction with the damage may result in noticeable fall in signal amplitude. In the present study, feasibility of generating Lamb wave modes in submerged FRP sheets has been experimentally explored by varying the incident angle (θ) of the transducers in PT configuration.
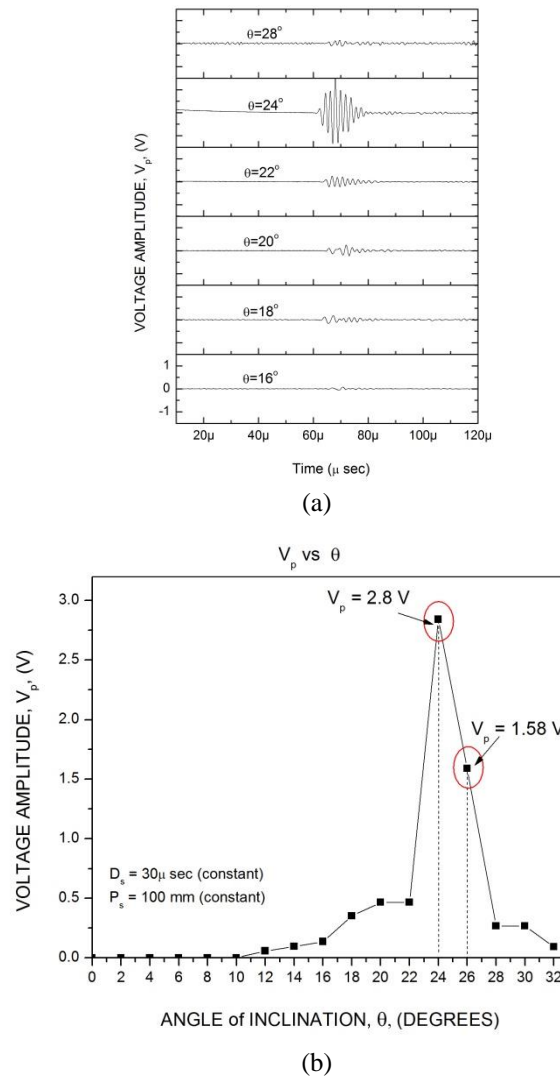
Fig. 4 (a) PT signatures at different angles of incidence and (b) Trends of V_p (0°- 32°)

Both the probes were placed with equal inclination (θ) and D_s with respect to the submerged FRP. During this study, P_s was kept as 100 mm for all values of θ. PT signatures were recorded by varying θ in steps of 2° starting with 0° as shown in Fig. 4(a). On the other hand, Fig. 4(b) shows the variation of received signal voltage amplitudes (V_p) with varying θ. No signal was detected by the receiver probe when θ varied from 0° to 10°. With further increase in θ (10° -16°), traces of ultrasonic signals were observed in PT signatures. Distinctive signals with sharp peak were observed when θ varied from 18° to 24° (Fig. 4(a)). However, with further increase in θ, the

voltage amplitude reduced sharply and no signal could be observed at higher values of θ (i.e., beyond 32°). This may be attributed to total reflection of the incident energy into the surrounding water. Thus, Figs. 4 (a) and 4(b) suggest that the inclination of the probes of 24° to vertical yields a UT signal with good fidelity that can be exploited for effective health monitoring purposes.

2.3 Selection of optimum propagation span (P_s)

Amplitude of signal for a given θ and D_s value is dependent upon the span travelled by the guided wave (P_s) through the submerged FRP specimen. As the Lamb waves travels through submerged specimen, it loses energy continuously to the surrounding water resulting in fall of signal strength as shown in Figs. 5 (a) and 5(b). Longer propagation span shall lead to weak signal amplitude whereas; shorter spans shall result in longer inspection times for a given specimen. So it is important to choose a suitable P_s so that signal fidelity and inspection time can be optimally balanced. Figs. 5(b) and 5(c) shows the variation of received signal strengths with varying Ps, while keeping other experimental parameters (θ = 24°, t_s = 30 μs) fixed. Fig. 5(b) shows PT signatures for P_s in the range of 120 – 200 mm. Received signal shows good signal fidelity that can be utilized for effective health monitoring of FRP laminates.

In Fig. 5(c), value of V_p (2.8 V) at P_s = 100 mm is found to be consistent with V_p (2.8 V) in Fig. 4 at θ = 24° thus, ensuring the repeatability of the experimental procedure. Fig. 5(c) suggests that propagation span (P_s) in the range of 100-150 mm, yields PT signals with V_p that can be exploited for health monitoring purposes at the given PR settings.

This study also provided another important wave propagation characteristic namely Group velocity (V_{gr}). As the P_s is increased from 90 mm to 210 mm in equal intervals of 10 mm, corresponding time of flight (TOF) of received signal is plotted. Fig. 6 shows that TOF varies linearly with respect to P_s. Group velocity of the propagating Lamb waves is given by inverse slope of this plot.

$$\frac{\Delta T}{\Delta D} (\text{Slope}) = 0.27923$$

$$V_{gr} = \frac{\Delta D}{\Delta T} = \frac{1}{\text{Slope}} = \frac{1}{0.27923} = 3.5813 \text{ m/sec} \qquad (2)$$

V_{gr} can also be determined theoretically by inputting the values of t_s, T_t and P_s in Eq. (3). Fig. 7 shows a recorded PT signature with P_s of 110 mm, $t_{s,t}$ and $t_{s,r}$ set at 30 μs.

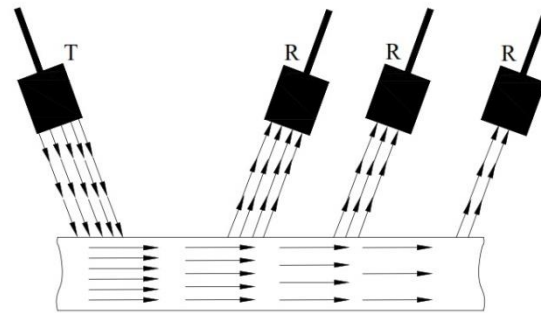$$V_{gr} = \frac{P_s}{T_t - \left(\frac{t_{s,t} + t_{s,r}}{2}\right)} \qquad (3)$$

where, P_s = propagation span between the transducers
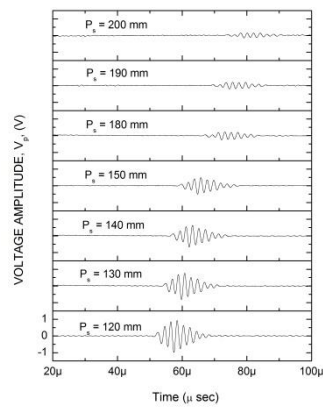T_t = Time of arrival of transmitted pulse in PT mode
$t_{s,t}$ = time of flight in water from transmitter (t)
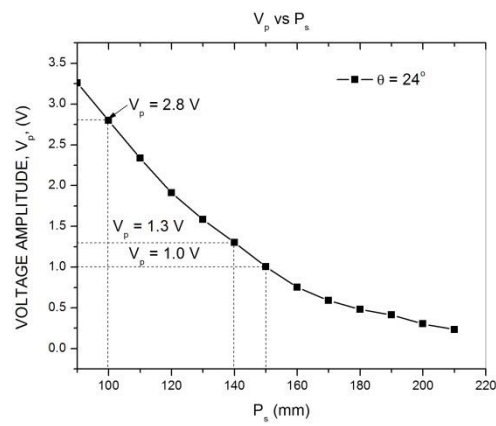$t_{s,r}$ = time of flight in water from receiver (r) probe

A single sharp peak appeared at T_t = 58.6 μs as seen in Fig. 7. Hence, the theoretically calculated group velocity of the Lamb waves is 3.84 m/sec which matches closely with that determined experimentally. The difference of 7% may be due to anisotropic behavior of the FRP sheet and experimental inaccuracy in setting the exact incident angles.

(a)

(b)

(c)

Fig. 5 (a) Pulse transmission loss over propagation span length, (b) Effect on PT signatures by varying propagation span and (c) Trends of transmitted pulses with increasing span
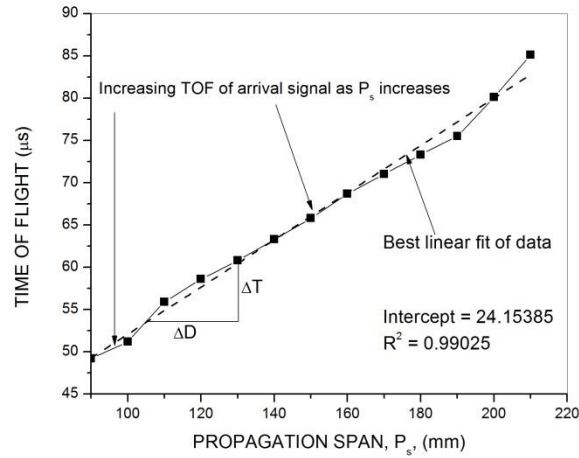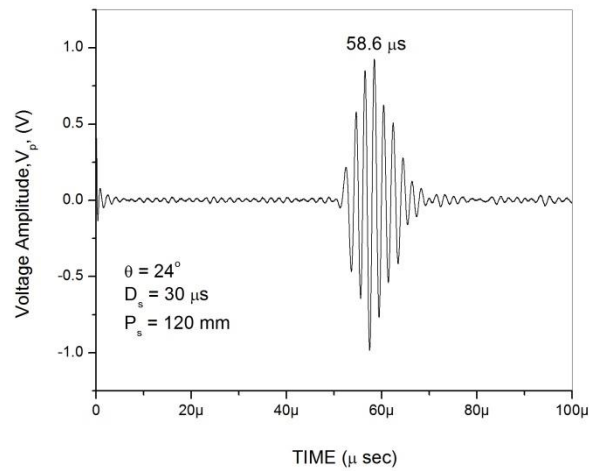
Fig. 6 Time of flight vs propagation span at 24° in healthy region

Fig. 7 Sample PT signature to calculate group velocity theoretically

The phase velocity of Lamb waves in FRP can also be calculated by using the Snell's law equation as mentioned in Eq. (1), where, the longitudinal velocity of wave in water is chosen to be 1.5 m/sec and θ = 24°.

$$Phase\ Velocity = \frac{1.5}{\sin^{-1}(24)} = 3.68\ m/sec \qquad (4)$$

The phase velocity and group velocity dispersion curves for the GFRP composites submerged in water are a complex mechanism to be modeled. However, sample phase velocity dispersion

curves have previously been reported in literature (Hayashi and Kawashima 2002, Hayashi *et al.* 2003, Hayashi and Rose 2003) by using a semi-analytical finite element method. It is stated that two fundamental modes propagate in the composite structure when using low frequency transducers up to 0.8 MHz.

A study by Hay *et al.* (2003) inspected the delaminated areas in composite skin-Nomex honeycomb specimens using ultrasonic guided waves. The sensitive mode was found experimentally by varying the frequency and phase velocity (in the range of 3500 – 4200 m/s) that effectively determined the delaminated zones in the composite structure. The experimental phase and group velocity results of the present study correlates well with those reported in literature. Therefore, the experimentally determined ultrasonic guided wave mode has been selected for the detection of manufacturing and usage defects in the composite laminates.

3. Specimen preparation

3.1 Preparation of FRP composite sheet

Advantex$^®$ E-glass fibers (GFs), woven roving fiber mat, WR310 was purchased from Owens Corning Inc., India. Commercial DGEBA-based epoxy resin and amine-based hardener (resin AIRSTONE 780E and hardener AIRSTONE 786H) were obtained from Dow Chemicals and used as the polymer matrix with a recommended resin to hardener weight ratio of 100:31. The fabrication of 2-ply glass fiber laminates was done using Vacuum Assisted Resin Infusion Molding (VARIM) technique. The glass fibers were placed on the top of the composite mold and were followed by a layer of peel ply, perforated foil, a runner mesh, breather cloth around the corners of the composite mold while covering the vacuum outlets. The sealant tape was pasted on the sides of the composite mold and the mold was sealed with vacuum bagging foil. An inlet pipe with a simple manifold was connected to the center of the glass fiber mat to allow equal distribution of resin throughout the fiber while one end was kept outside the vacuum foil for infusion. The vacuum was maintained at 1 – 2 mBar for 180 min after infusion. The recommended curing schedule was followed for 7 h at a 70℃. Glass fiber reinforced polymer composite (GFRP) sheet with dimensions of 600 mm x 600 mm x 0.7 mm of uniform thickness was prepared.

3.2 Defect detection using guided waves

3.2.1 Manufacturing defects in laminates

During manufacturing, defects are likely to occur due to experimental inaccuracies or external factors. In the present study, defects in the form of air voids and missing epoxy were seeded while manufacturing the composite laminate. During the preparation of GFRP in VARIM, the vacuum pump was switched off for 30 min prior to the complete curing of epoxy resin, so that patches of voids in the form of air gaps were seeded in the fiber-matrix interface. Also, to introduce missing epoxy defects in the sheet, a layer of runner mesh on glass fiber mat was removed at various locations resulting in resin deficit regions. A defect monitoring system using guided waves has been developed to detect these manufacturing and other service related damages in a composite sheet.

The nomenclature used for manufacturing defects and in-service damages in GFRP composite sheet are listed in Table 1 and also shown in Fig. 8.

Air gaps

The most important defect likely to occur in manufacturing of FRPs is "porosity" – the presence of voids. They are typically caused due to small air molecules between the glass fiber layers, malfunctioning of vacuum pump or due to the air entrapped during processing of resin and hardener. The air gaps would result in minimal stress transfer from the matrix to fibers and is thus a critical parameter that needs to be detected. It affects the interlaminar shear strength (ILSS) and severely mars the structural performance of specimen. The voids in the FRP are difficult to see with naked eye but become apparent when submerged in water. For the given specimen, air gaps were marked on the sheet as shown in Fig. 8. Various locations in the specimen illustrate the possibility of voids which are marked as A1- A4, and are also listed in Table 1. Ultrasonic pitch catch testing was carried out in the identified zones in the sheet to study the effect of air gaps on the signal fidelity. For the testing purposes, both the probes were placed in pitch catch arrangement at angle of incidence of 24° and signal was recorded at a propagation span of 110 mm and 120 mm. The presence and extent of air gaps in the composite can be estimated ultrasonically by comparing the PT signal amplitude at the defective locations vis-à-vis healthy signal amplitude. Initially, PT signatures were first recorded in the adjacent healthy region adjoining the air gaps and then the transducers were moved along X-Y axis to record the ultrasonic signal at marked air gap locations in the sheet. The voltage amplitude of the received signals was normalized with respect to healthy signals in-order to avoid any bias.

Missing epoxy

Another common manufacturing defect observed in the FRP sheets is the missing epoxy defect observed in poorly prepared composite sheets having patches of rich or deficient resin regions originating due to non-uniform spread of polymer matrix. This defect can be identified by carefully observing the FRP sheet and is indicated by an exposed glass fiber layer having no epoxy resin coating on it. Although, the resin is being infused into the mold through an efficient mechanism still, such defects occur during VARIM, possibly due to uneven mesh distribution (which assists the resin flow) or due to inhibition of resin flow by the inlet pipe etc. Missing epoxy defects induced during manufacturing of the sheet have been identified on the specimen as D1, D2, and D3 as shown in Fig. 8. On moving the two probes along X-axis of the tank, the marked regions with missing epoxy defects were found to be either normal (D1) or inclined (D2), to the propagating Lamb waves (i.e., X-direction of the FRP sheet). The PT signatures were recorded at the defective sites (D1 - D3) while keeping parameters such as θ, D_s, P_s and PR settings unchanged. For carrying out a comparative analysis on the same scale, the recorded voltage amplitudes were normalized with healthy voltage amplitude for each missing epoxy location.

3.2.2 Simulated usage defects

Due to various environmental and loading factors, degradation of the composites (in-service) takes place, which needs to be monitored periodically in order to avoid catastrophic failures. The internal defect such as material degradation and fiber breakage in FRPs may be attributed to numerous factors such as overloading, impact loads, fatigue, hygrothermal effects, over-heating, creep etc. Also, the penetration of moisture and other small molecules could degrade the interfacial properties due to the plasticization effect on resin. Additionally, the external defects like cracks, abrasion, notches, scratches etc. also affect the performance of FRP. These damages manifest in the form of delamination and debonding of the specimen, which results in lowering the mechanical properties such as stiffness and strength of the composites. In the present study, usage defects have

been simulated in the prepared composite sheet in the form of notches and surface defects.

Notches and surface defects

In this study, for both notch and surface defects, the effect of normal and oblique inclinations has been investigated by carrying out comparative analysis of their respective signal amplitudes with healthy signal. Initially, the PT signatures were recorded in the healthy region using the selected Lamb waves mode (at $\theta = 24^o$). Subsequently, a notch, N1, being 0.5 mm wide and with a depth of 25% of sheet thickness, normal to the Lamb waves (X-direction) was machined (Fig. 8) for which the ultrasonic signatures were recorded. Further, the transducers were slightly moved along X-axis (of the tank) to record the ultrasonic signal for another notch, N2, having width same as N1, but, with an increased depth of 50% of the sheet thickness. Besides this, a notch, N3, at 60° to the horizontal with 1.5 mm width and 25% thickness of the sheet was also machined (Fig. 8) and PT signature were recorded for the same.

Apart from the above mentioned notches, FRP composites may also encounter surface defects called abrasions (like scratches, material degradation) during its service conditions which over longer time period significantly affect the strength and stiffness of the composites. The presence of surface defects in FRPs can be monitored using the non-contact technique discussed in this paper. Initially, the ultrasonic signals were recorded in the healthy region by exciting the selected Lamb wave mode travelling along X-direction (as labeled on submerged FRP sheet). Subsequently, material losses due to surface abrasion or scratches were seeded on the specimen by scooping out the material using a cutter. These surface defects machined on the sheet have been identified as S1, S2, S3 and S4 (Fig. 8).

Table 1 Nomenclature for manufacturing defects and in-service damages in GFRP composite sheet as shown in Fig. 8

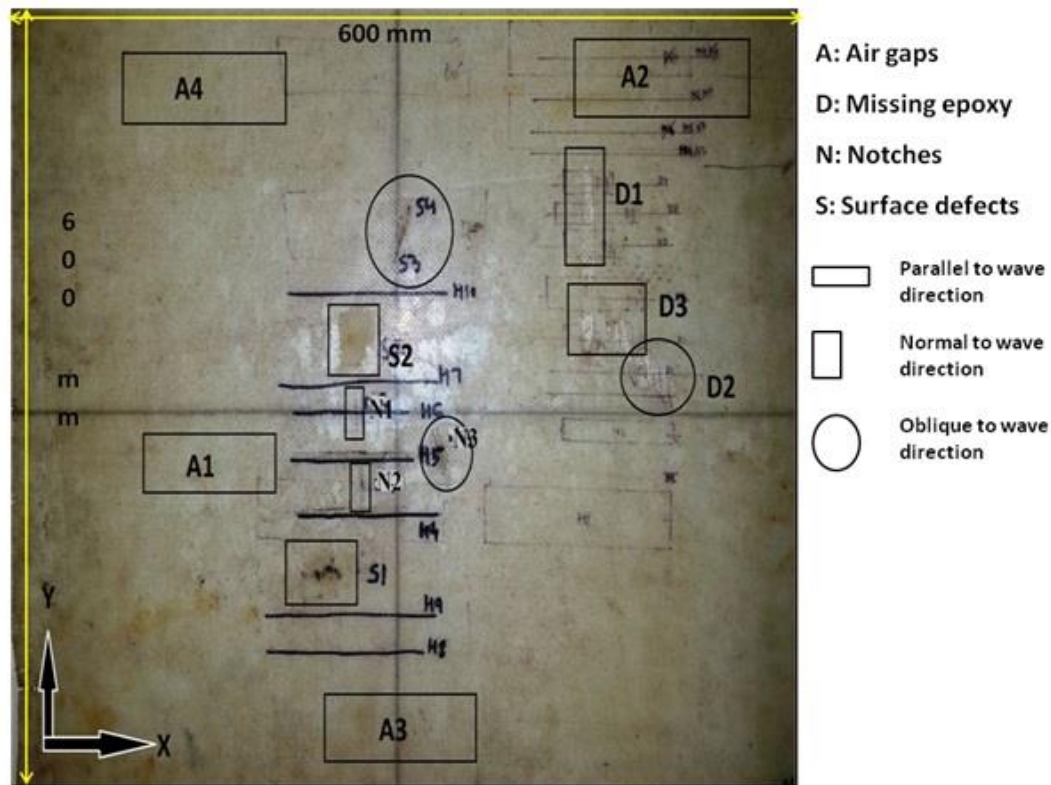| Type of defect	Nomenclature	Details of defect type
Air voids	A1,A2,A3, A4	Air gaps
Missing epoxy	D1	Missing epoxy (normal to propagating wave)
	D2	Missing epoxy (oblique to propagating wave)
	D3	Missing epoxy (normal and oblique)
Notches	N1	25% depth, normal to propagating wave
	N2	50% depth, normal to propagating wave
	N3	25% depth, oblique to propagating wave
Surface defects	S1	Material removed parallel to propagating wave, dimensions of the defect: width = 4 cm and length 2 cm
	S2	Normal to the direction of wave and having dimensions: width 2 cm and length 3cm with more amount of material removed from the sheet as compared to S1.
	S3	Surface material was scratched obliquely to the propagating wave with dimensions: 2 mm width and 35 mm length
	S4	Surface material was scratched obliquely to the propagating wave and cut through FRP sheet

Fig. 8 Photograph of GFRP sheet with manufacturing defects (air gaps and missing epoxy) and in-service

The location S1 depicts a region parallel to the propagating wave (with dimensions: width = 4 cm and length = 2 cm) as compared to S2, which is normal to the direction of wave and has a larger amount of material removed from the sheet compared to S1 (with dimensions: width = 2 cm and length = 3 cm). Further surface defects at an obliquity were also marked on locations S3 and S4 both with same dimensions (i.e. width = 2 mm and length = 35 mm) but having varied depths of 60% and 90%, respectively were seeded at 60° (with respect to X-axis) in the FRP sheet. UT signatures were similarly taken at healthy as well as S1- S4 locations.

3.3 Methodology

This section briefly describes the procedure to perform non-destructive testing of the FRP sheets to study the effect of material defects or imperfections seeded in FRP laminates during manufacturing or while in service on the signal fidelity. The baseline signatures in healthy zones are recorded by generating specific Lamb wave mode in FRP sheet by arranging the probes in pitch catch orientation.

To ensure good signal fidelity and repeatability of results, the time of flight for the probes (in pitch catch orientation) was set at 30 µs in PE mode. In-order to record ultrasonic signals,

experimental parameters such as $\theta = 24^{o}$ and PR settings were kept constant, while the span length (P_s) of 110 mm and 120 mm was considered throughout the experimental investigation. The PT signatures were recorded for healthy regions in the submerged FRP sheet. Subsequently by moving the transducers along X-axis, the signal produced during interaction of Lamb waves, with damages and defective zones (as discussed in Section 4.2) was recorded and compared vis-à-vis to healthy region.

4. Results & discussion

For the FRP composites, during the propagation of Lamb waves, PT signatures are likely to be affected when they encounter any type of defect in the submerged specimen. Effect of manufacturing as well as usage defects in the FRPs has been investigated and discussed in the following sections.

4.1 Presence of air gap

The air gets entrapped in the sheet either during the resin preparation or due to vacuum leakage during the fabrication, results in a significant decrease in interlaminar shear strength of composite. Air gaps in a composite sheet does not produce a discrete reflection but scatters the ultrasonic wave in different directions, also resulting in transmission loss. The PT signatures and the V_n trends have been obtained for selected Lamb wave mode for healthy and varying lengths of air gap patches in the FRP sheet. Fig. 9 shows PT signatures recorded over healthy region and air gap locations (A1-A4) in the submerged specimen. The PT signature for the healthy and defected region highlights that after interaction with the air voids in the composite sheet, the signal remains unaltered and no mode conversion is observed. But a drop of 32% in the voltage amplitude is seen after interaction with A1 while, the shape of the arriving peak and TOF remains unaltered. Voids in the sheet tend to change the acoustic impedance and consequently less energy is transmitted to the receiving transducer which is indicated by drop in the signal amplitude. Quantitative change in signal strength vis-à-vis voids in the FRP specimen with respect to healthy signal is an indication of the extent of air gap.

The trend of V_n vs air gap locations (A1 − A4), seen in Fig. 10, illustrates a decrease in the V_n of the recorded signal as the Lamb waves propagates through the air gaps compared to healthy region. Some locations have shown more drop in the received signal as compared to others which could possibly be due to the varying amount of air present in the fiber-matrix interface. The drop in signal strength vis-à-vis healthy signal is observed to be approximately 32%, 45%, 55% and 56%, at locations A1, A2, A3 and A4, respectively with $\theta = 24^{o}$ and P_s = 110 mm. A similar trend has been witnessed by further increasing the span length (P_s) between the probes to 120 mm. Moreover, there is a linear decrease in V_n as the length of air gap increases. Interestingly, for similar length of air gap patches at locations A3 and A4, a negligible change in signal strength is witnessed which suggests the repeatability of the experimental results.

Hence, it is observed that as the length of air gap increases, V_n of the recorded signal diminishes. These variations highlight the efficacy of selected Lamb wave mode for detecting manufacturing defects like air voids in the fiber-matrix interface by drop in signal amplitudes as the waves interact with the air gaps.
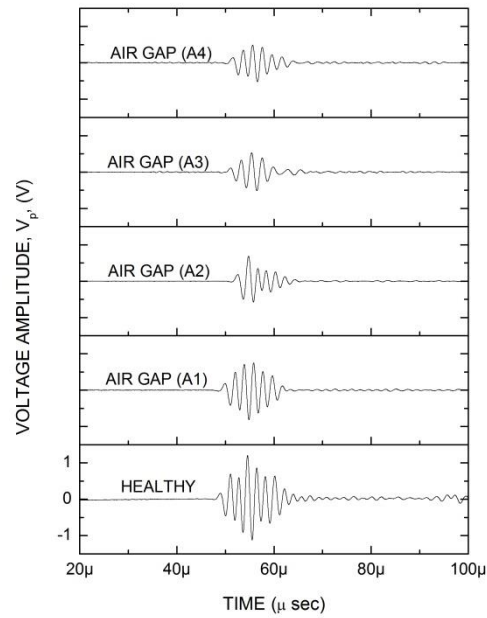
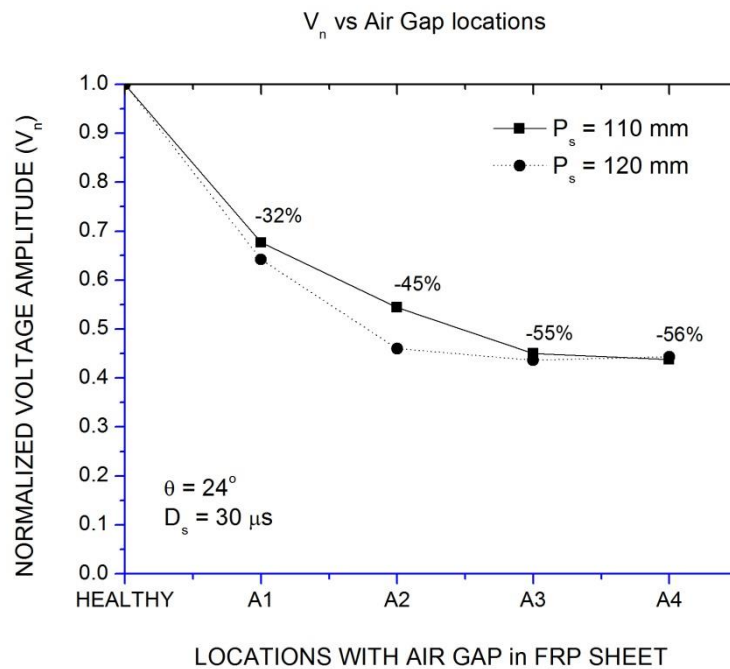Fig. 9 Effect on PT signatures with air gap locations (A1-A4) vis-à-vis healthy region

Fig. 10 Trends of normalized transmitted pulse voltages with presence of air gaps

4.2 Missing epoxy

The missing epoxy refers to the non-uniform distribution of resin over the fiber sheets. The effect on PT signature with missing epoxy locations (D1- D3) compared to healthy signal is shown in Fig. 11. While, Fig. 12 shows the decreasing trend observed in the UT signals with missing epoxy defect vis-à-vis healthy region in the composite sheet. It is observed that as the Lamb waves propagate in the regions with missing epoxy, voltage amplitude of the received signal diminishes. The missing epoxy regions were oriented in different directions such as normal, oblique and both normal and oblique to the direction of Lamb waves (i.e., along X-direction in sheet). Comparison of healthy region with respect to the missing epoxy defect in terms of normalized voltage amplitude indicates that the transmitted pulse amplitude varies with the direction of the defect.

The initial fall in V_n for normal missing epoxy defect (D1) is 40% of the healthy voltage amplitude and is 70% for oblique epoxy defect (D2). This fall is considerably significant as compared to the fall in V_n experienced for location D3, consisting of both normal and oblique defect. From Fig. 12 it is clear that by changing the propagation span between the receiver and the transmitter there is no change in the type of signal recorded and a similar trend is followed for all the missing epoxy locations studied. The drop in V_n is steepest at D3 being 78% for P_s of 110 mm and increases to 81% for P_s of 120 mm as shown in Fig. 12.

Ultrasonic Lamb waves are sensitive to manufacturing defects like air gaps and missing epoxy created during manufacturing of laminate and hence can be effectively used for identifying internal defects in the FRP sheets immediately after they are manufactured and cured. This technique can go a long way in improving the quality of the composite laminates where they are put to use or applied. The developed non-contact and non-invasive Lamb wave technique can be effectively used for damage monitoring and quantifying the defects induced during manufacturing of FRPs.
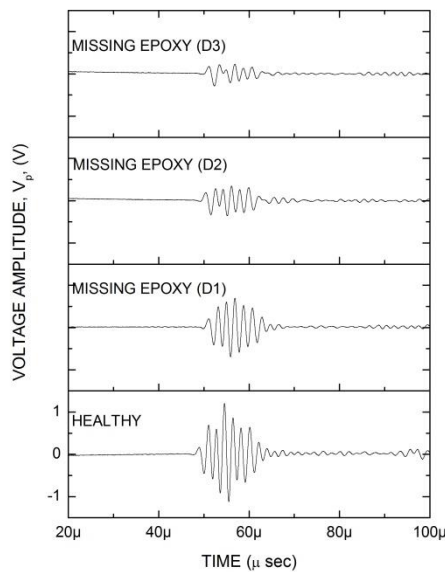

Fig. 11 Effect on PT signatures with missing epoxy (D1-D3) vis-à-vis healthy signal
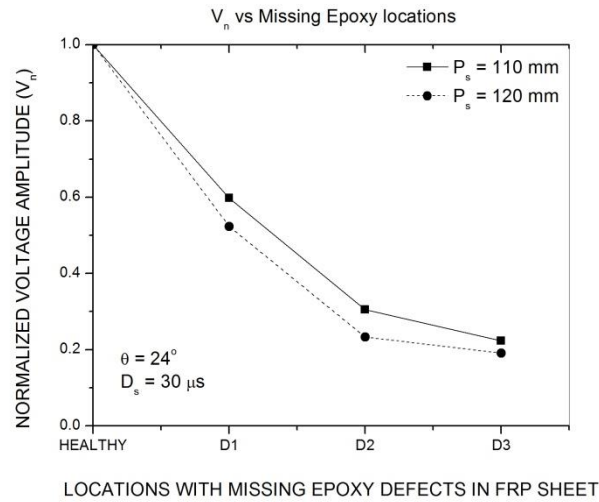
Fig. 12 Trends of normalized transmitted pulse voltages with different missing epoxy defects

4.3 Notches and surface defects

In the prepared FRP sheets, effect of increasing notch depth and orientation of notch on ultrasonic signal strength has been investigated with respect to healthy signal. Fig. 13 shows the effect of machined notches of varying depths on the received UT signal amplitude vis-à-vis their respective healthy signals.
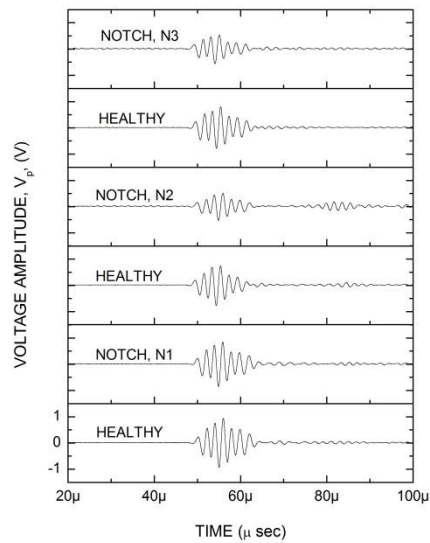

Fig. 13 Effect on PT signatures with notches (N1-N3) vis-à-vis healthy signal
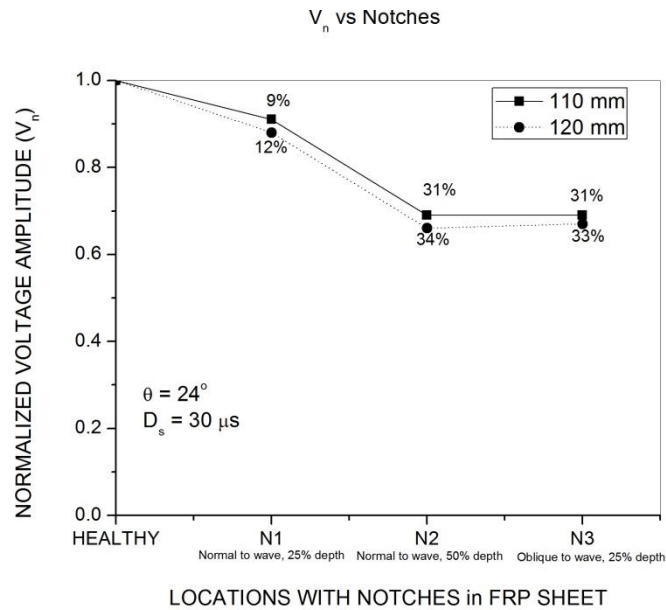
Fig. 14 Trends of normalized transmitted pulse voltages with different notch depth and orientation

Fig. 14 clearly illustrates that as the percentage depth of notch increases, voltage amplitude of UT signal decreases. It is possibly due to the increased reflection and scattering of the Lamb waves from the vertical wall of the notch. The fall in voltage amplitude for 25% notch depth (N1) is 8.9% and is 31% for 50% notch depth (N2), as compared to their respective healthy regions. However, an inclined notch (N3) with same depth as N1 i.e., 25%, shows 31% drop in V_n with respect to its healthy signal. Hence, significant drop in the received signal amplitude is observable as the depth and inclination of the notch increases. Similar trend is followed at $P_s = 120$ mm with a fall in voltage amplitude of 12%, 34% and 33% for N1, N2 and N3, respectively which establishes the repeatability of the experimental set-up. Hence, this technique gave a fall indication of the effect of notches on the amplitude of the signal transmitted. This establishes the efficacy of guided waves in identifying defects like internal cracks, or fatigue cracks in FRP sheets simulated as notches in the present study.

As discussed earlier, the exposure of composite sheets to marine environment for longer durations results in material degradation. The degraded material sites act as stress concentration points resulting in quick crack initiation, followed by crack propagation and final rupture of the composite. In the present study, this was investigated by scooping out the surface material at various locations and in different orientations with respect to the wave propagation in the FRP sheet and its effect on the received ultrasonic signals was also investigated.

For the healthy regions identified in the submerged FRP sheet, PT signatures were characterized by good signal fidelity and subsequently compared with surface defect locations as shown in Fig. 15.

However, in the regions with material loss, a significant drop in voltage of the transmitted signal was observed while the sharpness of the UT signal remained unaltered. At location S1, a drop of 42% in V_n is observed while, at S2 a drop of 69% in V_n is seen compared to the

corresponding V_n recorded at healthy region (Fig. 16). The significant fall at S2 is likely due to two reasons: direction of surface defect (normal) with respect to the propagating wave and excess removal of material from the surface of FRP sheet as compared to S1. However, when the surface defect is machined at an angle, the fall in V_n is relatively higher as indicated by uniform slope of the corresponding trend in Fig. 16. This fall is observed to be steepest at S4 (94%) due to the excess removal of material from the specimen, visualized as a deeper cut (by naked eye) near that region. It is therefore, possible that the guided wave propagated through the sheet but, only a small portion of the transmitted wave was received by the receiver probe. On further increasing the P_s to 120 mm, the behavior of V_n follows a similar trend as observed for P_s = 110 mm. Therefore, the non-uniform loss of material from the surface results in signal attenuation due to the scattering of waves. It is well depicted by fall in the voltage amplitudes of the received pulse with increasing loss in material degradation. PT scanning of the composite sheet in submerged state with varying material degradation due to usage indicates that any material degradation in the FRP sheet is well picked up by fall in transmitted signal strength and can be easily picked up. The guided wave methodology has the potential and ability to pick up degradation due to usage of imperfections in the prepared FRP sheets marked by fall in signal strength.

Carefully generated specific Lamb wave modes can be used to characterize the presence of manufacturing defects and in-service damages and quantify the defects in submerged fiber polymer composites by implementing the present in-situ, non-contact and non-invasive ultrasonic technique.
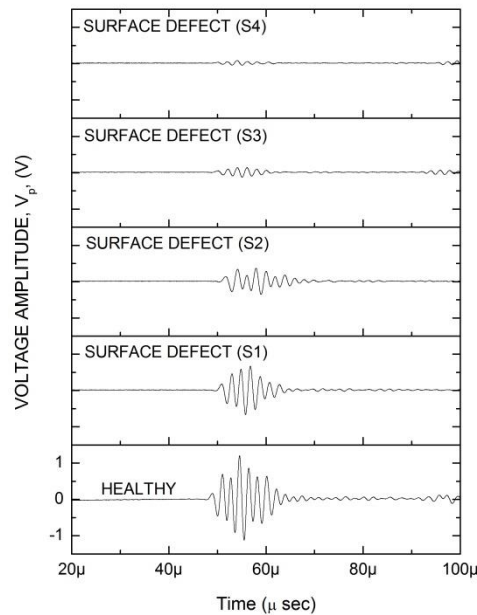

Fig. 15 Effect on PT signatures with surface defect (S1-S4) vis-à-vis healthy signal
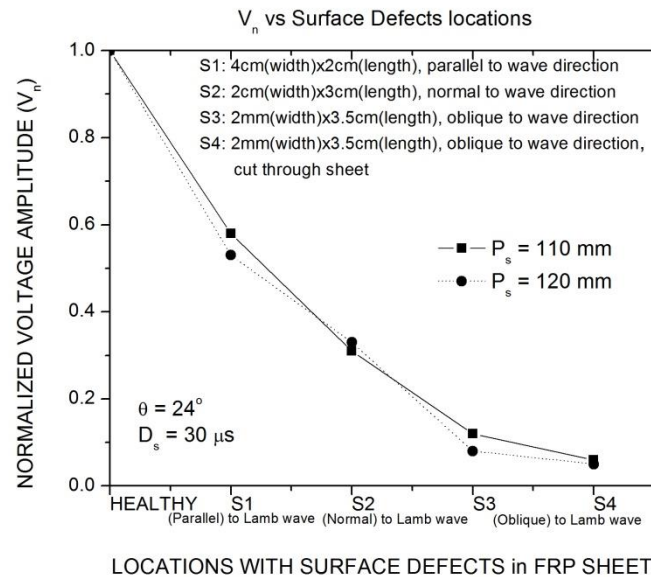
Fig. 16 Trends of normalized transmitted pulse voltages with different surface defects

5. Conclusions

The present study successfully establishes the efficacy of ultrasonic guided waves in submerged composite laminates to develop a non-contact, in-situ and non-invasive damage monitoring system which can find wide application in marine and other naval structures. These structures can be monitored without the necessity of removal from their current assemblies, by using a pair of mobile immersion probes generating the specific Lamb wave modes. Lamb waves can pick up air gaps and missing epoxy defects in the newly prepared FRP sheets. The transmitted signal strength falls when the Lamb wave interacts with these defects. Interestingly, the sharpness and time of flight of the received signal remains unaffected by the presence of these defects in FRPs. Also, the Lamb waves are sensitive to degradation in the FRP sheets due to its continual usage causing defects like notches, material degradation, surface discontinuities etc. The fall in voltage amplitude is an indicator of these defects in FRP sheets while in-service. Ultrasonic guided waves have sensitivity to both internal and external defects in two-ply GFRP composites and can be exploited as an effective damage monitoring technique; also has the potential to develop into an in-situ and non-invasive health monitoring tool. The sensitivity of different Lamb wave modes to specific defects will be investigated further.

Acknowledgments

References

Bagheri, A. and Rizzo, P. (2016), "Guided ultrasonic wave testing of an immersed plate with hidden defects", *Opt. Eng*., **55**(1), 011003-011003.

Ben, B.S., Ben, B.A., Vikram, K.A. and Yang, S.H. (2013), "Damage identification in composite materials using ultrasonic based Lamb wave method", *Measurement*, **46**, 904-912.

Benammar, A., Drai, R. and Guessoum, A. (2008), "Detection of delamination defects in CFRP materials using ultrasonic signal processing", *Ultrasonics*, **48**, 731-738.

Castaings, M. and Hosten, B. (2001), "Lamb and SH waves generated and detected by air-coupled ultrasonic transducers in composite material plates", *NDT&E Int*., **34**, 249-258.

Chaki, S., Harizi, W., Bourse, G. and Ourak, M. (2015), "Multi-technique approach for non destructive diagnostic of structural composite materials using bulk ultrasonic waves, guided waves, acoustic emission and infrared thermography", *Composites Part A*, **78**, 358-361.

Chakrapani, S.K. and Dayal, V. (2014), "The interaction of Rayleigh waves with delaminations in composite laminates", *J. Acoust. Soc. Am*., **135**(5), 2646-2653.

De Angelis, G., Meo, M., Almond, D.P., Pickering, S.G. and Angioni, S.L. (2012), "A new technique to detect defect size and depth in composite structures using digital shearography and unconstrained optimization", *NDT & E Int*., **45**(1), 91-96.

Harb, M.S. and Yuan, F.G. (2016), "Non-contact ultrasonic technique for Lamb wave characterization in composite plates", *Ultrasonics*, **64**, 162-169.

Hay, T.R. and Rose, J.L. (2002), "Guided wave testing optimization", *Mater. Eval*., **60**(10), 1239 -1344.

Hay, T.R., Wei, L. and Rose, J.L. (2003), "Rapid inspection of composite skin-honeycomb core strucutres with ultrasonic guided waves", *J. Compos. Mater*., **37**(10), 929-939.

Hayashi, T. and Kawashima, K. (2002), "Multiple reflections of lamb waves at a delamination", *Ultrasonics*, **40**,193-197.

Hayashi, T. and Rose, J.L. (2003), "Guided wave simulation and visualization by a semi-analytical finite element method", *Mater. Eval*., **61**(1), 75 - 79.

Hayashi, T., Rose, J.L., Kawashima, K. and Sun, Z. (2003), "Analysis of flexural mode focusing by a semi-analytical finite element method", *J. Acoust. Soc. Am*., **113**(3), 1241-1248.

Hong, K.M., Kang, Y.J., Choi, I.Y., Kim, S.J. and Lee, G.D. (2015), "Ultrasonic signal analysis according to laser ultrasound generation position for the detection of delamination in composites", *J. Mech. Sci. Technol.,* **29**(12), 5217-5222.

Hung, Y.Y., Luo, W.D., Lin, L. and Shang, H.M. (2000), "Evaluating the soundness of bonding using shearography", *Compos. Struct.*, **50**, 353-362.

Liu, L., Avioli, M.J. and Rose, J.L. (2001), "Incident angle selection for the guided wave inspection of pipe defects", *Insight*, **43**(2), 33-38.

Liu, X., Zhou, C. and Jiang, Z. (2012), "Damage localization in plate-like structure using built-in PZT sensor network", *Smart Struct. Syst*., **9**(1), 21-33.

Liu, Z.H., Yu, H.T., He, C.F. and Wu, B. (2013), "Delamination damage detection of laminated composite beams using air coupled ultrasonic transducers ", *Sci. China Phys. Mech. Astron*., **56**(7), 1269-1279.

Miao, X.T., Ye, L., Li, F.C., Sun, X.W., Peng, H.K., Lu, Y. and Meng, G. (2012), "A split spectrum processing of noise-contaminated wave signals for damage identification", *Smart Struct. Syst*., **10**(3), 253-269.

Moll, J., Torres-Arredondo, M.A. and Fritzen, C.P. (2012), "Computational aspects of guided wave based damage localization algorithms in flat anisotropic structures", *Smart Struct. Syst*., **10**(3), 229-251.

Na, W.B. and Kundu, T. (2002), "Underwater pipeline inspection using guided waves", *J. Press. Vess. Technol*., **124**, 196-200.

Palumbo, D., Tamborrino, R., Galietti, U., Aversa, P., Tatì, A. and Luprano, V.A.M. (2016), "Ultrasonic analysis and lock-in thermography for debonding evaluation of composite adhesive joints", *NDT&E Int*., **78**, 1-9 .

Pistone, E., Li, K. and Rizzo, P. (2013), "Noncontact monitoring of immersed plates by means of laser induced ultrasounds", *Struct. Health Monit.*, **12**(5-6), 549-565.

Pistone, E. and Rizzo, P. (2015), "On the use of an array of ultrasonic immersion transducers for the nondestructive testing of immersed plates", *Nondestruct. Test. Eval.*, **30**(1), 26-38.

Providakis, C.P., Triantafillou, T.C., Karabalis, D., Papanicolaou, A., Stefanaki, K., Tsantilis, A. and Tzoura, E. (2014), "Simulation of PZT monitoring of reinforced concrete beams retrofitted with CFRP", *Smart Struct. Syst.*, **14**(5), 811-830.

Putkis, O., Dalton, R.P. and Croxford, A.J. (2016), "The anisotropic propagation of ultrasonic guided waves in composite materials and implications for practical applications", *Ultrasonics*, **65**, 390-399.

Ramadas, C., Balasubramaniam, K., Joshi, M. and Krishnamurthy, C.V. (2011a), "Characterisation of rectangular type delaminations in composite laminates through B-and D-scan images generated using Lamb Waves", *NDT&E Int.*, **44**, 281-289.

Ramadas, C., Hood, A., Padiyar, J., Balasubramaniam, K. and Joshi, M. (2011b), "Sizing of delamination using time-of-flight of the fundamental symmetric lamb modes", *J. Reinf. Plast. Comp.*, **30**(10), 856-863.

Rizzo, P., Han, J.G. and Ni, X.L. (2010), "Structural health monitoring of immersed structures by means of guided ultrasonic waves", *J. Intel. Mat. Syst. Str.*, **21**(14), 1397-1407.

Sharma, S. and Mukherjee, A. (2014), "Damage detection in submerged plates using ultrasonic guided waves", *Sadhana*, **39**(5), 1009-1034.

Sharma, S. and Mukherjee, A. (2015a), "A non-contact technique for damage monitoring in submerged plates using guided waves", *J. Test. Eval.*, **43**(4), 1-16.

Sharma, S. and Mukherjee, A. (2015b), "Ultrasonic guided waves for monitoring corrosion in submerged plates", *Struct. Control Health Monit.*, **22**(1), 19-35.

Sihn, S., Kim, R.Y., Kawabe, K. and Tsai, S.W. (2007), "Experimental studies of thin-ply laminated composites", *Compos. Sci. Technol.*, **67**(6), 996 -1008.

Wilcox, P.D., Dalton, R.P., Lowe, M.J.S. and Cawley, P. (1999), "Mode and transducer selection for long range Lamb wave inspection", *Key Eng. Mater.*, **167-168**, 152 -161.

De Angelis, G., Dati, E., Bernabei, M. and Leccese, F. (2015), "Development on aerospace composite structures investigation using thermography and shearography in comparison to traditional NDT methods", *Metrology for Aerospace,* IEEE, Benevento.

Rizzo, P., Pistone, E. and Bagheri, A. (2015), "Guided ultrasonic waves for the NDT of immersed plates", *Emerging Technologies in Non-Destructive Testing VI: Proceedings of the 6th International Conference on Emerging Technologies in Non-Destructive Testing*, Brussels, May.

CC